ISSN 1392-1207. MECHANIKA. Vol. 32, No. 1, 2026: 5–12

Effect of Suction and Injection on the Time-Varying Flow Produced by an Oscillating Porous Disk and a Newtonian Fluid at Infinity Rotating about Parallel Axes

H. Volkan ERSOY
Department of Mechanical Engineering, Yildiz Technical University, 34349 Istanbul, Türkiye,
E-mail: hversoy@yildiz.edu.tr

https://doi.org/10.5755/j02.mech.38224

1. Introduction

The study of non-coaxial rotations, particularly involving porous boundaries, serves as a canonical configuration for understanding the complex momentum transfer mechanisms in rotating machinery. The physical relevance of this setup extends to various industrial and biological applications, such as hydrodynamic lubrication in non-aligned journal bearings, the operational stability of centrifugal pumps, and the fluid dynamics within biomedical oxygenators. Beyond industrial applications, the studied configuration has significant conceptual importance in the context of geophysical fluid dynamics. The interaction between an oscillating porous boundary and a fluid rotating at infinity directly relates to the dynamics of the Ekman boundary layer. In such systems, the presence of suction or injection significantly modifies the Ekman transport and the associated secondary flow patterns. Specifically, suction serves as a mechanism to suppress the thickness of the Ekman layer, thereby enhancing the stability of the rotational motion against unsteady periodic disturbances. This makes the present analytical model a valuable tool for understanding how boundary transpiration (suction/injection) can be used to control planetary-scale flow analogs or industrial vortex flows where non-coaxiality introduces complex inertial coupling.

The unsteady flow caused by the non-concentric rotation of a disk and a fluid at infinity, both sharing a common angular velocity, has captured the interest of numerous researchers. Kasiviswanathan and Rao [1] examined the time-dependent flow generated by a porous disk undergoing elliptical harmonic oscillations. Hayat et al. [2] investigated the periodic flow resulting from a single oscillating porous disk with superimposed suction or blowing. Guria et al. [3] derived an analytical solution for the time-varying Navier–Stokes equations, focusing on shear stresses and velocity distribution for the case of a porous disk. Erdoğan [4] investigated the unsteady flow generated by the eccentric rotation of a disk making non-torsional oscillation and the fluid at infinity as they are rotating in the concentric form. Hayat et al. [5] were the first to consider a non-Newtonian fluid and solved the problem for a porous disk interacting with a second grade fluid characterized by a small material modulus.

References [6–10] investigated the time-varying flows influenced by a magnetic field. Hayat et al. [6] examined the flow dynamics of a porous disk interacting with a Newtonian fluid. The flow corresponding to the generalized oscillations without torsion was analysed by Hayat et al. [7]. Hayat et al. [8] investigated how the Hall current affects the flow involving a porous disk. Hayat et al. [9] explored the flow for a second grade fluid having the small material modulus when the disk is porous. Wang and Wu [10] carried out a numerical analysis belonging to the flow of a third-order fluid and a disk with uniform suction or blowing. Recently, Lakshmi and Santhakumari [11] investigated the MHD flow resulting from non-concentric rotations of an oscillating porous disk and a viscous fluid at infinity, presenting a velocity distribution for this flow. They considered that both the disk and the fluid at infinity are rotating about a shared axis at the initial stage. Subsequently, Lakshmi and Santhakumari [12] investigated the impact of Hall effects on the same flow. Hussain [13] examined the MHD flow involving a porous disk and an oscillating fluid at infinity. As they are rotating about a shared axis, they begin rotating about distinct axes, with the fluid at infinity also oscillating. He provided the exact solutions of velocity field and shear stresses.

On the other hand, the unsteady flow resulting from the non-concentric rotation of a vertical disk and a fluid at infinity has been investigated under the influence of various factors by many researchers [14-20]. Mohamad et al. [14] investigated the simultaneous influence of heat and mass transfer on mixed convection flow of a viscous fluid over an oscillating disk in the vertical direction. Noranuar et al. [15] investigated the fluid dynamics and heat transfer for MHD Casson nanofluid in a porous medium induced by the non-coaxial rotation of a moving vertical disk. Noranuar et al. [16] analysed the transfer of heat and mass in Newtonian nanofluids within a porous medium with magnetohydrodynamic and radiation effects in the case of a moving vertical disk. Jabbar et al. [17] studied the mass transport under first-order chemical reaction conditions, considering thermal radiation effects, buoyancy, and both constructive and destructive chemical reactions in the presence of a Casson fluid in a rotating frame. The free convection flow of water-based carbon nanotubes was carried out by Noranour et al. [18]. Alqarni et al. [19] numerically simulated the flow of a Casson fluid over a vertical spinning disk, considering magnetic field, heat source, thermal radiation, second-order chemical reactions, buoyancy effect. Noranuar et al. [20] studied the mixed convection flow of a viscous fluid over an accelerating disk in a porous medium, incorporating radiative effects and the influence of a magnetic field.

Unlike the above studies, Ersoy [21, 22] considered the non-coaxial rotation as the initial motion. In Ref. [21], he analysed the time-dependent flow of a Newtonian fluid caused by a disk with non-torsional oscillation as the disk and the fluid at infinity are rotating eccentrically with the common angular velocity at the beginning of the oscillation motion. In Ref. [22], he extended this study to the magnetohydrodynamic flow.

This paper aims to extend the analysis in Ref. [21] to the case of a porous disk and presents the exact and periodic solutions of the velocity distribution and shear stresses for a Newtonian fluid. As the disk and the fluid at infinity are rotating non-coaxially at the outset, the disk starts to make oscillation without torsion in its own plane. The main goal of the paper is to study the effect of the suction and injection on the unsteady flow. Comparing the present results with the non-porous case, it is observed that suction acts as a stabilizing agent by suppressing the inertial effects of the non-coaxial rotation, whereas injection promotes the diffusion of oscillation-induced disturbances deeper into the fluid domain. The obtained exact solution is valid for all values of dimensionless time $t \geq 0$. In addition, a solution for the periodic motion occurred after the initial transients disappear is presented. It is shown that the flow reaches a periodic state more rapidly in both suction and injection cases.

The analytical expressions obtained via the Laplace transform method were evaluated and numerically computed using Wolfram Mathematica. The graphical representations and parametric analyses were generated using MATLAB in the velocity and shear stress distributions.

2. Basic Equations and Solution

Consider an incompressible Newtonian fluid over an infinite disk placed at $z = 0$. The z and z' axes separated by a distance ℓ characterize the axes of rotation of the disk and the fluid at infinity, both rotating at the common angular velocity Ω. At $t = 0$, the disk begins to oscillate within its own plane without torsion. The velocity vector of oscillation

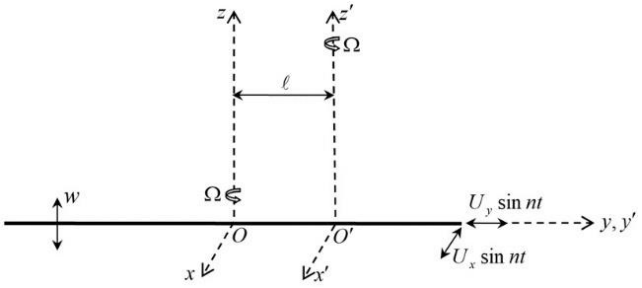

Fig. 1 Schematic diagram of the problem

has components $U_x \sin nt$ and $U_y \sin nt$ in the x and y directions, as seen in Fig. 1. Here n symbolizes the frequency of the oscillation.

The appropriate initial and boundary conditions are

$$u = -\Omega y + \hat{f}(z),\ v = \Omega x + \hat{g}(z),\quad \text{at } t = 0 \text{ for } z \geq 0; \tag{1}$$

$$u = -\Omega y + U_x \sin nt,\ v = \Omega x + U_y \sin nt,\quad \text{at } z = 0 \text{ for } t \geq 0; \tag{2}$$

$$u = -\Omega(y - \ell),\ v = \Omega x,\quad \text{at } z \to \infty \text{ for } t \geq 0, \tag{3}$$

where u and v are the velocity components along the x and y directions, $\hat{f}(z)$ and $\hat{g}(z)$ characterize the x and y components of the translational velocity vector of the steady flow before the beginning of the oscillation and are given by

$$\frac{\hat{f}(z)}{\Omega\ell} + i\frac{\hat{g}(z)}{\Omega\ell} = 1 - exp\left[\left(\frac{\rho w_0}{2\mu} - \sqrt{\frac{\rho^2 w_0^2}{4\mu^2} + i\frac{\rho\Omega}{\mu}}\right)z\right]. \tag{4}$$

Here, ρ is the density of the fluid, μ is the dynamic viscosity of the fluid, and w_0 is the constant axial velocity.

It is appropriate to propose a velocity field in the following form:

$$u = -\Omega y + f(z,t),\quad v = \Omega x + g(z,t),\quad w = w_0 \tag{5}$$

which satisfy the continuity equation. Here, $w_0 > 0$ corresponds to injection and $w_0 < 0$ corresponds to suction.

By means of the Navier-Stokes equations, the governing equation is obtained as follows:

$$\mu\frac{\partial^2 \Gamma}{\partial z^2} - \rho w_0 \frac{\partial \Gamma}{\partial z} - \rho\frac{\partial \Gamma}{\partial t} - i\rho\Omega\Gamma = -i\rho\Omega^2\ell. \tag{6}$$

Here, $\Gamma(z, t) = f(z, t) + ig(z, t)$.

The dimensionless governing equation and the corresponding conditions are reduced to the following equations:

$$\frac{\partial^2 F}{\partial \zeta^2} - 2\sqrt{2}\,b\frac{\partial F}{\partial \zeta} - 2\frac{\partial F}{\partial \tau} - 2iF = 0, \tag{7}$$

$$F(\zeta,0) = -exp\left[\sqrt{2}\left(b - \sqrt{b^2 + i}\right)\zeta\right] \text{ for } \zeta \geq 0, \tag{8}$$

$$F(0,\tau) = V\sin k\tau - 1 \text{ for } \tau \geq 0, \tag{9}$$

$$F(\infty,\tau) = 0 \text{ for } \tau \geq 0, \tag{10}$$

where

$$F(\zeta,\tau) = \frac{\Gamma(z,t)}{\Omega\ell} - 1,\quad \zeta = \sqrt{\frac{\rho\Omega}{2\mu}}\,z,\quad \tau = \Omega t,$$
$$b = \frac{w_0}{2\sqrt{\Omega\mu/\rho}},\quad V_x = \frac{U_x}{\Omega\ell},\quad V_y = \frac{U_y}{\Omega\ell},$$
$$V = V_x + iV_y,\quad k = \frac{n}{\Omega}. \tag{11}$$

2.1. Exact solution

Let us denote by $\bar{F}(\zeta, s)$ the Laplace transform of F with respect to t.

$$\bar{F}(\zeta,s) = \int_0^\infty F(\zeta,\tau)exp(-s\tau)d\tau. \tag{12}$$

When we have taken the Laplace transforms of Eq. (7) and Eqs. (9)-(10), we obtain

$$\bar{F}''-2\sqrt{2}b\bar{F}'-2(s+i)\bar{F}=$$
$$=2exp\left[\sqrt{2}\left(b-\sqrt{b^2+i}\right)\zeta\right], \quad (13)$$

$$\bar{F}(0)=\frac{Vk}{s^2+k^2}-\frac{1}{s}, \quad (14)$$

$$\bar{F}(\infty)=0. \quad (15)$$

The solution of Eq. (13) subject to Eqs. (14) and (15) becomes

$$\bar{F}=\frac{Vk}{s^2+k^2}exp\left[\sqrt{2}\left(b-\sqrt{b^2+i+s}\right)\zeta\right]-$$
$$-\frac{1}{s}exp\left[\sqrt{2}\left(b-\sqrt{b^2+i}\right)\zeta\right]. \quad (16)$$

Taking the Laplace inversion of Eq. (16) yields

$$\tilde{f}(\zeta,\tau)+i\tilde{g}(\zeta,\tau)=1-exp\left[A_0(\zeta)\right]+$$
$$+\frac{Vi}{4}\begin{Bmatrix} exp\left[C_1(\zeta,\tau)\right]erfc\left[B_1(\zeta,\tau)\right]+\\ +exp\left[C_2(\zeta,\tau)\right]erfc\left[B_2(\zeta,\tau)\right]-\\ -exp\left[C_3(\zeta,\tau)\right]erfc\left[B_3(\zeta,\tau)\right]-\\ -exp\left[C_4(\zeta,\tau)\right]erfc\left[B_4(\zeta,\tau)\right] \end{Bmatrix}, \quad (17)$$

where

$$\tilde{f}(\zeta,\tau)=\frac{f(z,t)}{\Omega\ell},\quad \tilde{g}(\zeta,\tau)=\frac{g(z,t)}{\Omega\ell},$$
$$A_0(\zeta)=\sqrt{2}\left(b-\sqrt{b^2+i}\right)\zeta,$$
$$B_1(\zeta,\tau)=\frac{\sqrt{2}\zeta-2\tau\sqrt{b^2+i(1-k)}}{2\sqrt{\tau}},$$
$$C_1(\zeta,\tau)=\sqrt{2}\left(b-\sqrt{b^2+i(1-k)}\right)\zeta-ik\tau,$$
$$B_2(\zeta,\tau)=\frac{\sqrt{2}\zeta+2\tau\sqrt{b^2+i(1-k)}}{2\sqrt{\tau}},$$
$$C_2(\zeta,\tau)=\sqrt{2}\left(b+\sqrt{b^2+i(1-k)}\right)\zeta-ik\tau,$$
$$B_3(\zeta,\tau)=\frac{\sqrt{2}\zeta-2\tau\sqrt{b^2+i(1+k)}}{2\sqrt{\tau}},$$
$$C_3(\zeta,\tau)=\sqrt{2}\left(b-\sqrt{b^2+i(1+k)}\right)\zeta+ik\tau,$$
$$B_4(\zeta,\tau)=\frac{\sqrt{2}\zeta+2\tau\sqrt{b^2+i(1+k)}}{2\sqrt{\tau}},$$
$$C_4(\zeta,\tau)=\sqrt{2}\left(b+\sqrt{b^2+i(1+k)}\right)\zeta+ik\tau. \quad (18)$$

Here, $\tilde{f}(\zeta,\tau)$ and $\tilde{g}(\zeta,\tau)$ symbolize the x and y components of the dimensionless translational velocity.

We get the shear stress components as follows:

$$\tilde{T}_{xz}(\zeta,\tau)+i\tilde{T}_{yz}(\zeta,\tau)=$$
$$=-\sqrt{2}\left(b-\sqrt{b^2+i}\right)exp\left[A_0(\zeta)\right]+$$
$$+\frac{Vi}{4}\begin{Bmatrix} exp\left[C_1(\zeta,\tau)\right]M_1(\zeta,\tau)+\\ +exp\left[C_2(\zeta,\tau)\right]M_2(\zeta,\tau)-\\ -exp\left[C_3(\zeta,\tau)\right]M_3(\zeta,\tau)-\\ -exp\left[C_4(\zeta,\tau)\right]M_4(\zeta,\tau) \end{Bmatrix}, \quad (19)$$

where

$$\tilde{T}_{xz}(\zeta,\tau)=\frac{T_{xz}(z,t)}{\sqrt{\mu\rho\Omega^3/2\ell}},$$
$$\tilde{T}_{yz}(\zeta,\tau)=\frac{T_{yz}(z,t)}{\sqrt{\mu\rho\Omega^3/2\ell}},$$
$$M_1(\zeta,\tau)=\sqrt{2}\left(b-\sqrt{b^2+i(1-k)}\right)erfc\left[B_1(\zeta,\tau)\right]-$$
$$-\sqrt{\frac{2}{\pi\tau}}exp\left[-B_1^2(\zeta,\tau)\right],$$
$$M_2(\zeta,\tau)=\sqrt{2}\left(b+\sqrt{b^2+i(1-k)}\right)erfc\left[B_2(\zeta,\tau)\right]-$$
$$-\sqrt{\frac{2}{\pi\tau}}exp\left[-B_2^2(\zeta,\tau)\right],$$
$$M_3(\zeta,\tau)=\sqrt{2}\left(b-\sqrt{b^2+i(1+k)}\right)erfc\left[B_3(\zeta,\tau)\right]-$$
$$-\sqrt{\frac{2}{\pi\tau}}exp\left[-B_3^2(\zeta,\tau)\right],$$
$$M_4(\zeta,\tau)=\sqrt{2}\left(b+\sqrt{b^2+i(1+k)}\right)erfc\left[B_4(\zeta,\tau)\right]-$$
$$-\sqrt{\frac{2}{\pi\tau}}exp\left[-B_4^2(\zeta,\tau)\right]. \quad (20)$$

Here, $\tilde{T}_{xz}(\zeta,\tau)$ and $\tilde{T}_{yz}(\zeta,\tau)$ represent the dimensionless shear stresses within the fluid.

The effects of suction and injection on the dimensionless translational velocity for specific values of the dimensionless time τ are indicated in Figs. 2-3. It is noteworthy that in the long-time regime ($t\to\infty$), the transient effects dissipate, and the fluid motion transitions into a purely periodic state.

The space curves generated by the centres of rotation of the fluid layers in each horizontal plane are indicated in Fig. 4.

Figs. 5-6 reveal how the suction and injection affect the dimensionless shear stresses at the disk throughout the entire temporal evolution.

2.2. Periodic solution

For a solution belonging to the periodic flow, we can take into consideration the following form:

$$F(\zeta,\tau)=F_0(\zeta)+F_1(\zeta)cos\,k\tau+F_2(\zeta)sin\,k\tau, \quad (21)$$

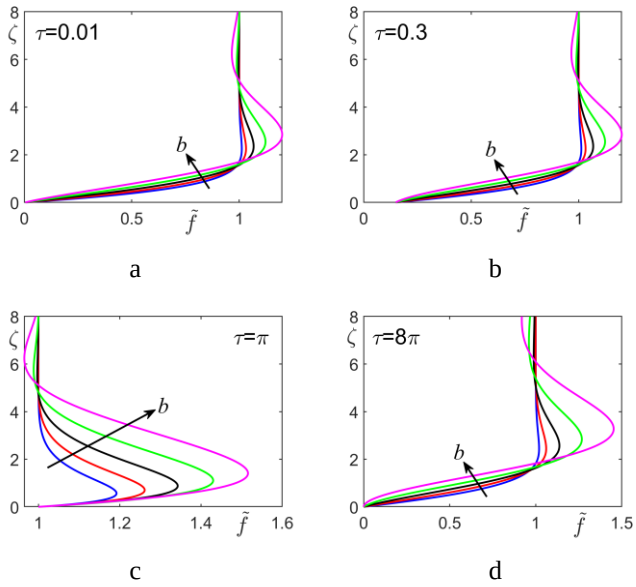

Fig. 2 Variation of $\tilde{f}$ with ζ for: a – $\tau = 0.01$, b – $\tau = 0.3$, c – $\tau = \pi$, d – $\tau = 8\pi$ ($k = 0.5$, $V_x = 1$, $V_y = 1$, $b = -0.4, -0.2, 0, 0.2, 0.4$)

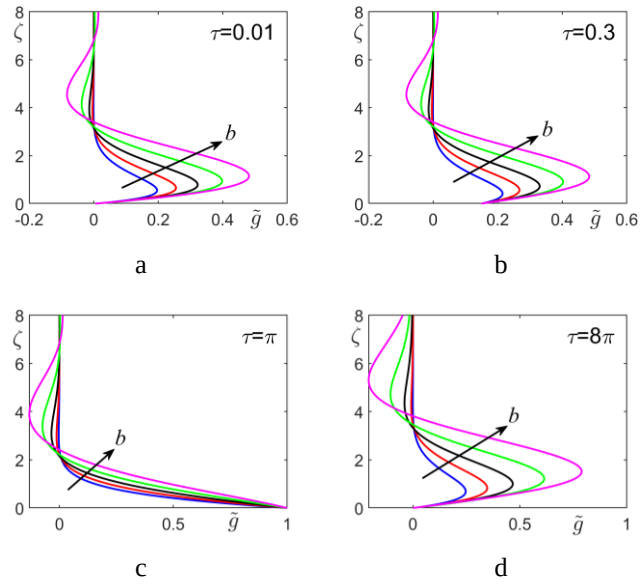

Fig. 3 Variation of $\tilde{g}$ with ζ for: a – $\tau = 0.01$, b – $\tau = 0.3$, c – $\tau = \pi$, d – $\tau = 8\pi$ ($k = 0.5$, $V_x = 1$, $V_y = 1$, $b = -0.4, -0.2, 0, 0.2, 0.4$)

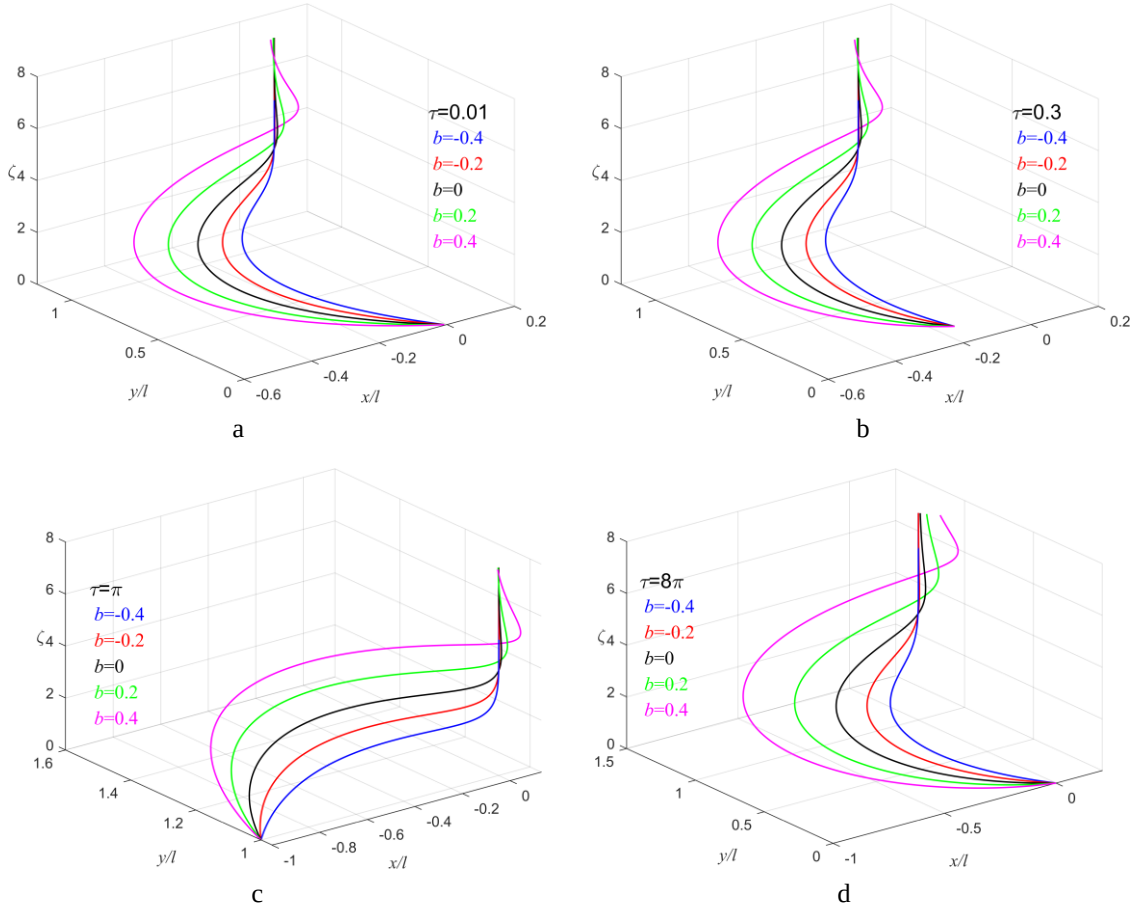

Fig. 4 Space curves formed by points with only vertical velocity: a – $\tau = 0.01$, b – $\tau = 0.3$, c – $\tau = \pi$, d – $\tau = 8\pi$ ($k = 0.5$, $V_x = 1$, $V_y = 1$), where $l = \ell$

where $F_0(\zeta)$ corresponds to the case of $n = 0$. Putting Eq.(21) in Eq. (7), one obtains:

$$F_0'' - 2\sqrt{2}bF_0' - 2iF_0 = 0, \tag{22}$$

$$F_1'' - 2\sqrt{2}bF_1' - 2kF_2 - 2iF_1 = 0, \tag{23}$$

$$F_2'' - 2\sqrt{2}bF_2' + 2kF_1 - 2iF_2 = 0, \tag{24}$$

with

$$F_0(0)=-1,\quad F_0(\infty)=0,$$
$$F_1(0)=0,\quad F_1(\infty)=0,$$
$$F_2(0)=V,\quad F_2(\infty)=0. \tag{25}$$

The solutions of Eqs. (22)-(24) subject to Eq. (25) give

$$\tilde{f}(\zeta,\tau)+i\tilde{g}(\zeta,\tau)=1-exp\left[A_0(\zeta)\right]+$$
$$+\frac{iV}{2}\left\{exp\left[K_1(\zeta)\right]-exp\left[K_2(\zeta)\right]\right\}cos\,k\tau+$$
$$+\frac{V}{2}\left\{exp\left[K_1(\zeta)\right]+exp\left[K_2(\zeta)\right]\right\}sin\,k\tau \tag{26}$$

and

$$\tilde{T}_{xz}(\zeta,\tau)+i\tilde{T}_{yz}(\zeta,\tau)=-\sqrt{2}\left(b-\sqrt{b^2+i}\right)exp\left[A_0(\zeta)\right]+$$
$$+\frac{iV}{2}\left\{\begin{matrix}\sqrt{2}\left(b-\sqrt{b^2+i(1-k)}\right)exp\left[K_1(\zeta)\right]-\\-\sqrt{2}\left(b-\sqrt{b^2+i(1+k)}\right)exp\left[K_2(\zeta)\right]\end{matrix}\right\}cos\,k\tau+\frac{V}{2}\left\{\begin{matrix}\sqrt{2}\left(b-\sqrt{b^2+i(1-k)}\right)exp\left[K_1(\zeta)\right]+\\+\sqrt{2}\left(b-\sqrt{b^2+i(1+k)}\right)exp\left[K_2(\zeta)\right]\end{matrix}\right\}sin\,k\tau, \tag{27}$$

where

$$K_1(\zeta)=\sqrt{2}\left(b-\sqrt{b^2+i(1-k)}\right)\zeta,$$
$$K_2(\zeta)=\sqrt{2}\left(b-\sqrt{b^2+i(1+k)}\right)\zeta. \tag{28}$$

The periodic solution, representing the long-time regime, is consistently recovered from the general exact solution as the transient terms associated with the complementary error functions vanish in the asymptotic limit ($t\to\infty$).

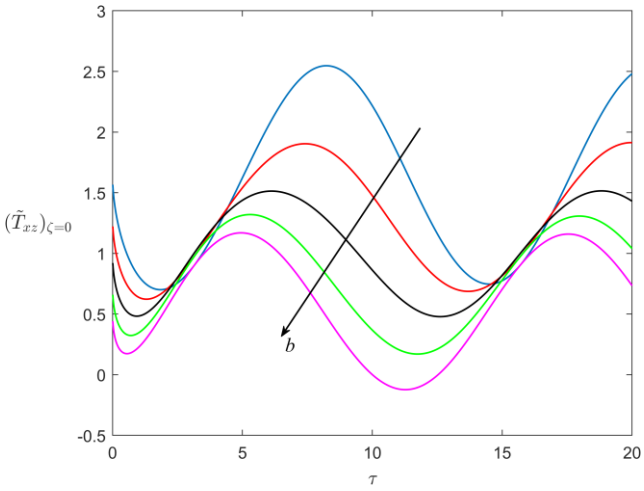

Fig. 5 Variation of $(\tilde{T}_{xz})_{\zeta=0}$ with τ (k = 0.5, V_x = 1, V_y = 1, b = –0.4, –0.2, 0, 0.2, 0.4)

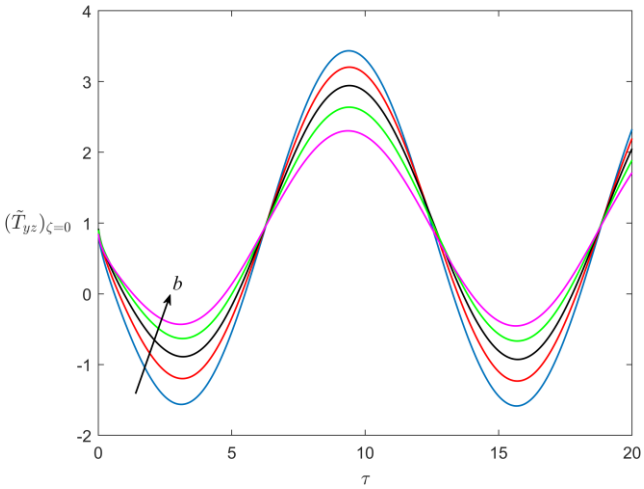

Fig. 6 Variation of $(\tilde{T}_{yz})_{\zeta=0}$ with τ ($k=0.5$; $V_x=1$; $V_y=1$; $b=-0.4,-0.2,0,0.2,0.4$)

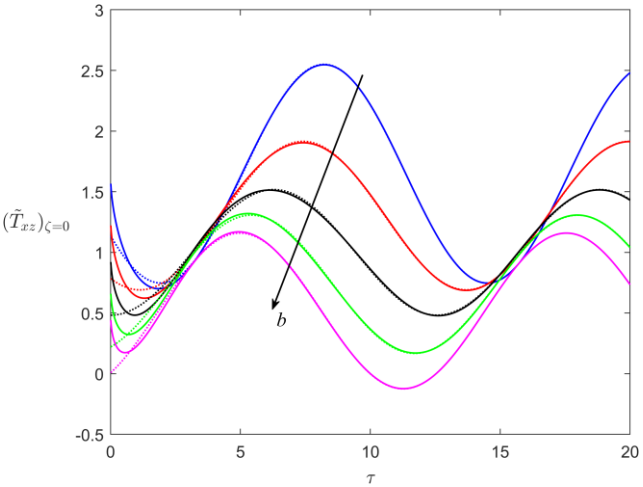

Fig. 7 Comparison of exact solution and periodic solution for the variation of $(\tilde{T}_{xz})_{\zeta=0}$ with τ (k = 0.5, V_x = 1, V_y = 1, b = –0.4, –0.2, 0, 0.2, 0.4) solid – exact, dot – periodic

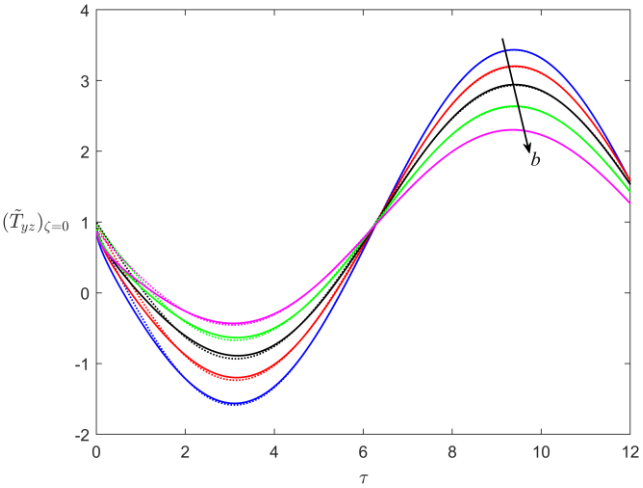

Fig. 8 Comparison of exact solution and periodic solution for the variation of $(\tilde{T}_{yz})_{\zeta=0}$ with τ (k = 0.5, V_x = 1, V_y = 1, b = –0.4, –0.2, 0, 0.2, 0.4) solid – exact, dot – periodic

Figs. 7-8 show the comparison of the exact and periodic solutions for the dimensionless shear stresses at the disk when the disk is subjected to the suction and injection.

3. Results and Discussion

In this paper, a disk subjected to a uniform suction ($b < 0$) or injection ($b > 0$) and the fluid at infinity are in rotation with the common angular velocity about two vertical parallel axes perpendicular to the disk at the initial time. The disk begins to oscillate without torsion in its horizontal plane. An exact solution derived by the Laplace transform method in addition to a periodic solution are presented for the velocity field and shear stresses at the disk.

Here, it is discussed how the suction parameter acts as a stabilizer by constraining the momentum diffusion, whereas injection leads to a boundary layer thickening effect that enhances the interaction between the primary and secondary flow components.

Figs. 2-3 show the variations of the dimensionless x and y components of the translational velocity with the suction/injection parameter (b) for some specific time values. As it is clearly seen, the imposition of suction has the tendency to reduce the velocity but the imposition of injection leads to an opposite effect on the velocity. The boundary layer gets thinner with the increase of the suction whereas the presence of injection makes the boundary layer thicker.

Due to the nature of the motion, the fluid layer in each plane parallel to the disk rotates around a central point with an angular velocity Ω. The trajectories of the central points are represented by curves in space (Fig. 4). The coordinates of this central point are found by $x/\ell = -V_y \sin k\tau$ and $y/\ell = V_x \sin k\tau$ at the disk and are specified by $x/\ell = 0$ and $y/\ell = 1$ at infinity. As time increases, the coordinates on the disk plane change due to sinusoidal oscillations, but this change is independent of the suction/injection parameter. In the suction case, the conditions $x/\ell \approx 0$ and $y/\ell \approx 1$ are satisfied in regions closer to the disk, whereas in the injection case they are met farther away. As a result, the length of the space curves decreases as suction intensifies, while the length of the curves increases as injection becomes stronger.

Figs. 5-6 represent the influence of suction/injection parameter (b) on the shear stresses at the disk. Increasing suction leads to a greater increase in the values of the shear stresses whereas injection acts in the opposite manner. Suction increases the amplitude of the oscillations, whereas an opposite behaviour is noticed for injection. It is clear from these figures that the fluid moves periodically at large values of time.

The difference between the exact solution and periodic solution for the shear stresses at the disk is shown in Figs. 7-8. In these figures, it is explicitly demonstrated how the transient terms derived from the Laplace transform inverse decay exponentially as $t \to \infty$, leaving only the periodic boundary layer solution. While the exact solution remains applicable for the complete range of dimensionless time, the periodic solution is not suitable in the initial transient regime. However, the two solutions give the same results as the time goes by.

4. Conclusions

This paper focuses on the effects of the suction and injection on the time-varying flow of a classical viscous fluid caused by the rotation of an oscillating porous disk and the fluid at infinity as they are rotating eccentrically with the same angular velocity at the initial stage. The following observations are made.

- It is observed that the suction or injection through the disk significantly change the flow field.
- When a uniform suction is applied, a reduction is observed in the translational velocity. But the reverse effect is observed for the case of injection.
- As intensity of suction grows, the length of the space curves described by the points possessing only axial velocity decreases; when injection intensity is increased, the opposite effect occurs. In both cases, the centre of the rotating layers approaches the vertical line intersecting the point ($x = 0$, $y = 0$) while moving away from the disk. This condition occurs in regions closer to the disk with increasing applied suction. The same condition is observed in regions further away from the disk with imposed injection.
- It is seen that the boundary layer becomes thinner for increasing suction and thickens for increasing injection.
- An increase in suction causes a rise in the values of the shear stresses but injection has an opposite effect on them.
- As the suction/injection parameter approaches zero ($b \to 0$), our exact solution reduces precisely to the classic results reported for non-porous disks [21].

Acknowledgements

The author gratefully acknowledges the anonymous reviewers for their insightful comments and constructive suggestions.

References

1. **Kasiviswanathan, S.R.; Rao, A.R.** 1987. An unsteady flow due to eccentrically rotating porous disk and a fluid at infinity, International Journal of Engineering Science 25(11-12): 1419-1425. https://doi.org/10.1016/0020-7225(87)90020-6.
2. **Hayat, T; Asghar, S; Siddiqui, A.M.** 1999. Unsteady Flow of an Oscillating Porous Disk and a Fluid at Infinity, Meccanica 34(4): 259-265. https://doi.org/10.1023/A:1004751322961.
3. **Guria, M; Das, B.K.; Jana, R.N.** 2007. Oscillatory flow due to eccentrically rotating porous disk and a fluid at infinity, Meccanica 42(5): 487-493. https://doi.org/10.1007/s11012-007-9071-9.
4. **Erdoğan, M.E.** 2000. Flow induced by non-coaxial rotation of a disk executing non-torsional oscillations and a fluid rotating at infinity, International Journal of Engineering Science 38(2): 175-196. https://doi.org/10.1016/S0020-7225(99)00017-8.
5. **Hayat, T.; Ellahi, R.; Asghar, S.; Siddiqui, A.M.** 2004. Flow induced by non-coaxial rotation of a porous disk executing non-torsional oscillations and a second grade fluid rotating at infinity, Applied Mathematical Modelling 28(6): 591-605. https://doi.org/10.1016/j.apm.2003.10.011.
6. **Hayat, T.; Zamurad, M.; Asghar, S.; Siddiqui, A.M.**

2003. Magnetohydrodynamic flow due to non-coaxial rotations of a porous oscillating disk and a fluid at infinity, International Journal of Engineering Science 41(11): 1177-1196.
https://doi.org/10.1016/S0020-7225(03)00004-1.

7. **Hayat, T.; Ellahi, R.; Asghar, S.** 2004. Unsteady periodic flows of a magnetohydrodynamic fluid due to non-coaxial rotations of a porous disk and a fluid at infinity, Mathematical and Computer Modelling 40(1-2): 173-179.
https://doi.org/10.1016/j.mcm.2003.09.035.
8. **Hayat, T.; Ellahi, R.; Asghar, S.** 2008. Hall effects on unsteady flow due to non-coaxially rotating disk and a fluid at infinity, Chemical Engineering Communications 195(8): 958-976.
https://doi.org/10.1080/00986440801906575.
9. **Hayat, T.; Ellahi, R.; Asghar, S.** 2007. Unsteady magnetohydrodynamic non-Newtonian flow due to non-coaxial rotations of disk and a fluid at infinity, Chemical Engineering Communications 194(1): 37-49.
https://doi.org/10.1080/00986440600642868.
10. **Wang, Y.; Wu, W.** 2007. Time-dependent magnetohydrodynamic flow induced by non-coaxial rotations of a non-torsionally oscillating porous plate and a third-order fluid at infinity, Mathematical and Computer Modelling 46(9-10): 1277-1293.
https://doi.org/10.1016/j.mcm.2007.01.005.
11. **Lakshmi, R.; Santhakumari, A.** 2020. MHD flows due to non-coaxial rotations of porous disk and a viscous fluid at infinity: Graphical solutions using Matlab, Advances in Mathematics: Scientific Journal 9(11): 9287-9301.
https://doi.org/10.37418/amsj.9.11.33.
12. **Lakshmi, R.; Santhakumari, A.** 2021. The effects of hall current on the flow due to the oscillating rotating porous disk with a viscous fluid at infinity: Graphical solutions using Matlab, Advances in Mathematics: Scientific Journal 10(5): 2491-2514.
https://doi.org/10.37418/amsj.10.5.15.
13. **Hussain, Z.** 2021. Unsteady MHD flow due to eccentric rotations of a porous disk and an oscillating fluid at infinity, Zeitschrift für Angewandte Mathematik und Mechanik 101(11): e202000369.
https://doi.org/10.1002/zamm.202000369.
14. **Mohamad, A.Q.; Khan, I.; Shafie, S.; Isa, Z.M.; Ismail, Z.** 2018. Non-coaxial rotating flow of viscous fluid with heat and mass transfer, Neural Computing and Applications 30(9): 2759-2769.
https://doi.org/10.1007/s00521-017-2854-6.
15. **Noranuar, W.N.N.; Mohamad, A.Q.; Shafie, S.; Khan, I.; Jiann, L.Y.; Ilias, M.R.** 2021. Non-coaxial rotation flow of MHD Casson nanofluid carbon nanotubes past a moving disk with porosity effect, Ain Shams Engineering Journal 12(4): 4099-4110.
https://doi.org/10.1016/j.asej.2021.03.011.
16. **Noranuar, W.N.N.; Mohamad, A.Q.; Shafie, S.; Khan, I.; Jiann, L.Y.** 2020. Radiative Non-Coaxial Rotation of Magnetohydrodynamic Newtonian Carbon Nanofluid Flow in Porous Medium with Heat and Mass Transfer Effects, Journal of Nanofluids 9(4): 321-335.
https://doi.org/10.1166/jon.2020.1754.
17. **Jabbar, N.; Hafeez, M.B.; Askar, S.; Nazir, U.** 2021. Non-Coaxially Rotating Motion in Casson Martial along with Temperature and Concentration Gradients via First-Order Chemical Reaction, Energies 14(22): 7784.
https://doi.org/10.3390/en14227784.
18. **Noranuar, W.N.N.; Mohamad, A.Q.; Shafie, S.; Khan, I.** 2022. Unsteady free convection flow of water-based carbon nanotubes due to non-coaxial rotations of moving disk, Journal of Applied Science and Engineering 25(3): 401-410.
https://doi.org/10.6180/jase.202206_25(3).0005.
19. **Alqarni, M.M.; Bilal, M.; Allogmany, R.; Tag-Eldin, E.; Ghoneim, M.E.; Yassen, M.F.** 2022. Mathematical analysis of Casson fluid flow with energy and mass transfer under the influence of activation energy from a non-coaxially spinning disc, Frontiers in Energy Research 10: 986284.
https://doi.org/10.3389/fenrg.2022.986284.
20. **Noranuar, W.N.N.; Mohamad, A.Q.; Jiann, L.Y.; Shafie, S.; Ching, D.L.C.** 2022. Radiative non-coaxial rotating flow for viscous fluid over accelerated disk with MHD and porosity effects, Sains Malaysiana 51(8): 2669-2680.
http://doi.org/10.17576/jsm-2022-5108-25.
21. **Ersoy, H.V.** 2017. Unsteady flow due to a disk executing non-torsional oscillation and a Newtonian fluid at infinity rotating about non-coaxial axes. Sādhanā - Academy Proceedings in Engineering Sciences 42(3): 307-315.
https://doi.org/10.1007/s12046-017-0600-5.
22. **Ersoy, H.V.** 2019. Effect of magnetic field on the time-dependent flow due to a disk with non-torsional oscillation and a Newtonian fluid at infinity rotating about distinct axes, Sādhanā - Academy Proceedings in Engineering Sciences 44: 152.
https://doi.org/10.1007/s12046-019-1132-y.

H. V. Ersoy

EFFECT OF SUCTION AND INJECTION ON THE TIME-VARYING FLOW PRODUCED BY AN OSCILLATING POROUS DISK AND A NEWTONIAN FLUID AT INFINITY ROTATING ABOUT PARALLEL AXES

S u m m a r y

In this paper, the time-dependent flow of a Newtonian fluid generated by a porous disk performing oscillation without torsion and the fluid at infinity rotating about two different axes is considered. As the disk and the fluid at infinity are rotating non-coaxially at the beginning of the oscillation motion, the disk initiates oscillations without torsion within its own plane. The exact solutions for the velocity and shear stresses within the fluid are presented and the influences of the suction and injection are analysed. The results indicate that increasing suction leads to a reduction in the length of the space curves associated with points at which the velocity is purely axial, whereas increasing injection results in an elongation of the curves. The application of suction leads to a decrease in the boundary layer thickness whereas it increases with the implementation of injection. Furthermore, a periodic solution is presented, and the analysis confirms that the time required for the flow to become periodic is shorter for both suction and injection cases.

Keywords: Newtonian fluid, oscillating porous disk, eccentric rotation, exact solution, periodic flow.

Received July 26, 2025
Accepted February 20, 2026